

# Dinuclear Palladium(III) Complexes with a Single Unsupported Bridging Halide Ligand: Reversible Formation from Mononuclear Palladium(II) or Palladium(IV) Precursors\*\*

Julia R. Khusnutdinova, Nigam P. Rath, and Liviu M. Mirica\*

Along with the well-known involvement of Pd<sup>0</sup> and Pd<sup>II</sup> oxidation states in a large number of palladium-catalyzed reactions,<sup>[1]</sup> recent reports have proposed the intermediacy of less-common Pd<sup>IV</sup> and Pd<sup>III</sup> oxidation states in several chemical transformations.<sup>[2]</sup> Among these systems, dinuclear and mononuclear Pd<sup>III</sup> complexes have been shown to act as active intermediates in both two- and one-electron oxidative C–H functionalization and C–C bond formation reactions.<sup>[3–6]</sup> For example, dinuclear organometallic Pd<sup>III</sup> complexes stabilized by a Pd–Pd bond have been recently reported<sup>[3,7]</sup> and shown to be a catalytically competent alternative to mononuclear Pd<sup>IV</sup> species in carbon–heteroatom bond-formation reactions.<sup>[3,4]</sup> In this context, we have recently shown that mononuclear Pd<sup>III</sup> complexes stabilized by a tetradentate diazapyridinophane ligand can be isolated and have shown that they exhibit C–C bond-formation reactivity.<sup>[6]</sup> Continuing our work in the study of high-valent Pd complexes, we report herein novel cationic dinuclear Pd<sup>III</sup> and mononuclear Pd<sup>IV</sup> complexes supported by a common tridentate nitrogen-donor ligand, *N,N',N''*-trimethyl-1,4,7-triazacyclononane (Me<sub>3</sub>tacn). Moreover, we provide evidence for the involvement of a Pd<sup>III</sup> species in the Kharasch addition reaction and confirm the ability of Pd to catalyze one-electron radical reactions. In addition, the reported Pd<sup>III</sup> systems are the first group 10 d<sup>7</sup>–d<sup>7</sup> dinuclear complexes bridged by a single unsupported halide ligand and represent a model of the delocalized Pd<sup>III</sup>–X–Pd<sup>III</sup> electronic structure that has been proposed to exist in some –Pd–X–Pd–X– one-dimensional (1D) chains.<sup>[8]</sup>

While triazacyclonane (tacn)<sup>[9,10]</sup> and other tacn derivatives<sup>[11]</sup> have been employed in the synthesis of Pd complexes, only one complex, [(Me<sub>3</sub>tacn)Pd<sup>II</sup>(MeCN)<sub>2</sub>](PF<sub>6</sub>)<sub>2</sub>, has been reported for Me<sub>3</sub>tacn.<sup>[10]</sup> We have synthesized the Pd<sup>II</sup> complexes [(Me<sub>3</sub>tacn)Pd<sup>II</sup>X<sub>2</sub>] (X = Cl **1a**, X = Br **1b**) through

the reaction of Me<sub>3</sub>tacn with [(MeCN)<sub>2</sub>Pd<sup>II</sup>X<sub>2</sub>].<sup>[12]</sup> The X-ray structure analysis of **1a** reveals a square-planar arrangement of two Cl<sup>–</sup> ions and two N atoms around Pd, while the third N atom of Me<sub>3</sub>tacn is not in close proximity to the metal center (Figure 1a),<sup>[13]</sup> in contrast to the five-coordinate geometry

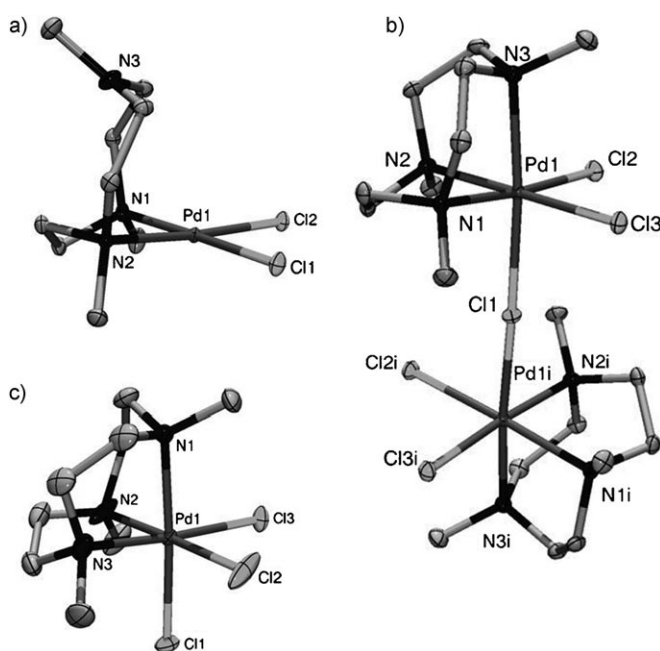


**Figure 1.** ORTEP representation (ellipsoids set at 50% probability) of a) **1a**, b) the cation of **2a**, and c) the cation of **3a**. Selected bond distances [Å] and angles [°]: **1a**: Pd1–N1 2.0736(5), Pd1–N2 2.0878(5), Pd1–Cl1 2.30651(18), Pd1–Cl2 2.32102(17). **2a**: Pd1–N1 2.094(2), Pd1–N2 2.105(2), Pd1–N3 2.273(2), Pd1–Cl2 2.3179(7), Pd1–Cl3 2.3224(7), Pd1–Cl1 2.4801(2), Cl1–Pd1i 2.4801(2), Pd1–Pd1i 4.931; Pd1–Cl1–Pd1i 167.47(4). **3a**: Pd1–N3 2.080(8), Pd1–N1 2.0806(16), Pd1–N2 2.093(8), Pd1–Cl1 2.302, Pd1–Cl2 2.308, Pd1–Cl3 2.308.

[\*] Dr. J. R. Khusnutdinova, Prof. Dr. L. M. Mirica  
Department of Chemistry, Washington University  
St. Louis, MO 63130 (USA)  
Fax: (+1) 314-935-4481  
E-mail: mirica@wustl.edu

Dr. N. P. Rath  
Department of Chemistry and Biochemistry  
University of Missouri–St. Louis (USA)

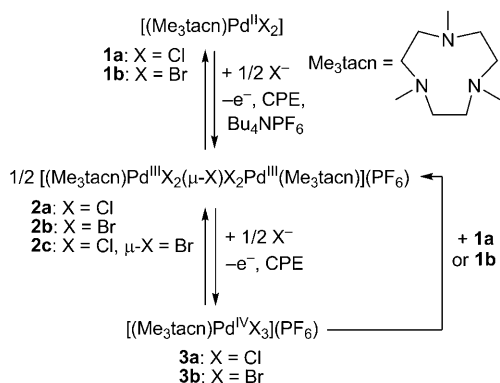
[\*\*] We thank the Department of Chemistry at Washington University and American Chemical Society Petroleum Research Fund (49914-DN13) for support. We also thank Prof. T. Daniel P. Stack for a gift of the ligand Me<sub>3</sub>tacn.

Supporting information for this article is available on the WWW under <http://dx.doi.org/10.1002/ange.201100928>.

observed for [(Me<sub>3</sub>tacn)Pd<sup>II</sup>(MeCN)<sub>2</sub>](PF<sub>6</sub>)<sub>2</sub>.<sup>[10]</sup> Cyclic voltammetry (CV) of both **1a** and **1b** in MeCN/Bu<sub>4</sub>NPF<sub>6</sub> reveals two closely-spaced waves at 0.05–0.17 V versus Fc<sup>+</sup>/Fc and additional waves at higher potentials, suggestive of oxidatively induced chemical reactions.<sup>[12,14]</sup>

Controlled potential electrolysis (CPE) at 0.3–0.4 V for both **1a** and **1b** leads to formation of a dark purple species in 60–70 % yields of isolated product after passing a charge corresponding to a one-electron oxidation. X-ray-quality crystals of the electrooxidation products obtained from MeCN/Et<sub>2</sub>O reveal the formation of dinuclear complexes

$[(\text{Me}_3\text{tacn})\text{Pd}^{\text{III}}\text{X}_2(\mu\text{-X})\text{Pd}^{\text{III}}\text{X}_2(\text{Me}_3\text{tacn})](\text{PF}_6)$  ( $\text{X} = \text{Cl}$  **2a**,  $\text{X} = \text{Br}$  **2b**), in which a single halide ion bridges the two Pd centers (Scheme 1 and Figure 1b; Supporting Information,



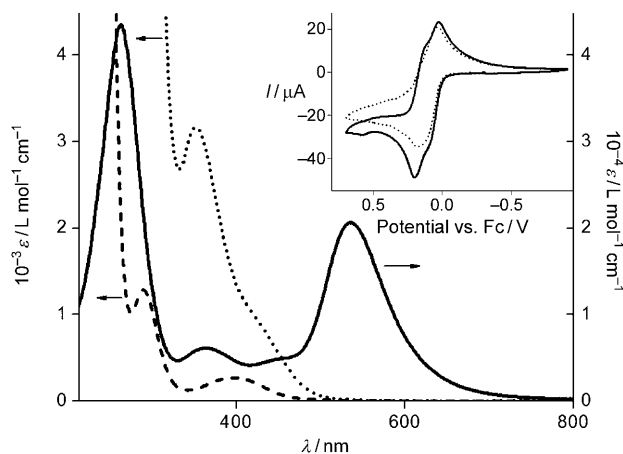
**Scheme 1.** Electrochemical synthesis of dinuclear  $\text{Pd}^{\text{III}}$  complexes and their interconversion to mononuclear  $\text{Pd}^{\text{III}}$  and  $\text{Pd}^{\text{IV}}$  complexes.

Figure S31).<sup>[13,15]</sup> Each metal center has a distorted octahedral geometry with two N atoms and the two terminal halides in the equatorial plane, while the third N atom of  $\text{Me}_3\text{tacn}$  and the bridging halide occupy the axial positions. The coordination geometry of Pd atoms and the overall charge of the dimer confirm the presence of  $\text{Pd}^{\text{III}}$  centers. To the best of our knowledge, complexes **2a** and **2b** are the first dinuclear  $\text{Pd}^{\text{III}}$  complexes that are not stabilized by a Pd–Pd bond.<sup>[3,7]</sup> Furthermore, this result suggests that stabilization of the  $\text{Pd}^{\text{III}}$  oxidation state can also be achieved by a tridentate N-ligand and does not require a rigid tetradentate ligand.<sup>[6]</sup>

The formation of dinuclear  $\text{Pd}^{\text{III}}$  complexes **2a** and **2b** from the mononuclear precursors **1a** and **1b** is intriguing. The circa 65% yield of product suggests that the bridging halide ion comes from another molecule of the  $\text{Pd}^{\text{II}}$  precursor.<sup>[16]</sup> Indeed, addition of 0.5 equiv of external halide leads to a simpler CV that shows only two closely spaced oxidative waves (Table 1; Supporting Information Figures S1–S4), and CPE at 0.3–0.4 V leads to formation of dark purple complexes **2a** and **2b** in higher yields (ca. 80%).<sup>[12,17]</sup> Interestingly, when  $\text{Br}^-$  was added to a solution of **1a**, the mixed halide complex  $[(\text{Me}_3\text{tacn})\text{Pd}^{\text{III}}\text{Cl}_2(\mu\text{-Br})\text{Pd}^{\text{III}}\text{Cl}_2(\text{Me}_3\text{tacn})](\text{PF}_6)$  (**2c**) formed (Scheme 1), as confirmed by X-ray crystallography (Support-

ing Information, Figure S31).<sup>[12]</sup> This observation suggests that the use of alternate exogenous ions can lead to  $\text{Pd}^{\text{III}}$  complexes with bridging ligands and altered electronic properties.<sup>[18]</sup> Complexes **2a–c** are structural models of the dinuclear unit found in  $-\text{M}-\text{X}-\text{M}-\text{X}-$  1D extended chains<sup>[8]</sup> in the average-valent Mott–Hubbard (MH)<sup>[8,19]</sup> state  $\text{M}^{\text{III}}-\text{X}-\text{M}^{\text{III}}$  (that is, a Robin–Day class III state).<sup>[20]</sup> The bridging halide ligand in **2a–c** is located at the midpoint between the two metal centers,<sup>[21]</sup> while the short Pd···Pd distances (**2a** 4.931 Å, **2b** 5.133 Å, **2c** 5.031 Å, Figure 1b; Supporting Information, Figure S31)<sup>[22]</sup> suggest an intimate orbital overlap between Pd and the bridging halide that is supported by the observed strong antiferromagnetic coupling between the unpaired  $d_{z^2}$  electrons of the two  $\text{Pd}^{\text{III}}$  centers,<sup>[23]</sup> which is typical for a delocalized MH state.<sup>[8,19b]</sup>

The UV/Vis spectra of complexes **2a–c** in MeCN reveal at least three intense absorption bands at 535–570 nm, 360–410 nm, and 260–280 nm, respectively (Table 1 and Figure 2).<sup>[24]</sup> Density functional theory (DFT) and time-



**Figure 2.** UV/Vis spectra of **1a** (----), **2a** (—), and **3a** (.....) in MeCN. Inset: CV of **1a** in the presence of 0.5 equiv  $\text{Cl}^-$  (.....) and 1 equiv  $\text{Cl}^-$  (—) in 0.1 M  $\text{Bu}_4\text{NPF}_6/\text{MeCN}$ .

dependent DFT (TD-DFT) calculations were employed in the assignment of these transitions. For **2a**, the 534 nm band exhibits an uncommonly large extinction coefficient ( $\epsilon = 21000 \text{ L mol}^{-1} \text{ cm}^{-1}$ ) and is assigned to an intermetallic Pd-to-Pd charge transfer (MMCT)<sup>[25]</sup> transition that is strongly mixed with a  $\mu\text{-Cl}$ -to-Pd CT transition (LMCT).<sup>[26]</sup> A similar assignment has been proposed for the low-energy transitions in  $\text{Pd}^{\text{III}}-\text{X}-\text{Pd}^{\text{III}}-\text{X}$  1D chains.<sup>[8]</sup> TD-DFT calculations support such an assignment by revealing a large oscillator strength for the HOMO to LUMO+1 MMCT transition, where the HOMO exhibits  $\sigma$ -bonding Pd– $\mu\text{-Cl}$  character and the LUMO+1 has antibonding Pd– $\mu\text{-Cl}$  character (Figure 3). Furthermore, the higher-energy bands can be assigned to a combination of bridging and terminal halide-to-Pd LMCT bands (for example, HOMO–10 and HOMO–12 to LUMO+1, respectively; Figure 3), as suggested previously<sup>[8]</sup> and supported by TD-DFT calculations.<sup>[12]</sup> As expected, the replacement of  $\text{Cl}^-$  with  $\text{Br}^-$  ligands for **2a** to **2c** to **2b** leads to

**Table 1:** Spectroscopic properties of dinuclear  $\text{Pd}^{\text{III}}$  complexes **2a–c**.

Complex	$E_{1/2}^{\text{III/III}}$ , $E_{1/2}^{\text{III/IV}}$ [mV] <sup>[a]</sup>	UV/Vis (MeCN) $\lambda$ [nm] ( $\epsilon$ [ $\text{L mol}^{-1} \text{ cm}^{-1}$ ])
<b>2a</b>	55, 163	534 (21 000), 449 (sh, 4900), 360 (6100), 260 (43 000)
<b>2b</b>	45, 171	570 (25 000), 411 (8900), 273 (47 000)
<b>2c</b>	65, 174 <sup>[b]</sup>	546 (17 000), 378 (6800), 262 (41 000)

[a] Potentials vs.  $\text{Fc}^+/\text{Fc}$  are measured by differential pulse voltammetry (DPV) for solutions of **1a** or **1b** in the presence of 1 equiv of  $\text{Cl}^-$  or  $\text{Br}^-$ , respectively, in 0.1 M  $\text{Bu}_4\text{NPF}_6/\text{MeCN}$ . Complexes **2a–c** show two oxidation waves at similar potentials (see the Supporting Information).

[b] Potentials are measured by DPV for a solution of **1a** in the presence of 1 equiv of  $\text{Br}^-$ .

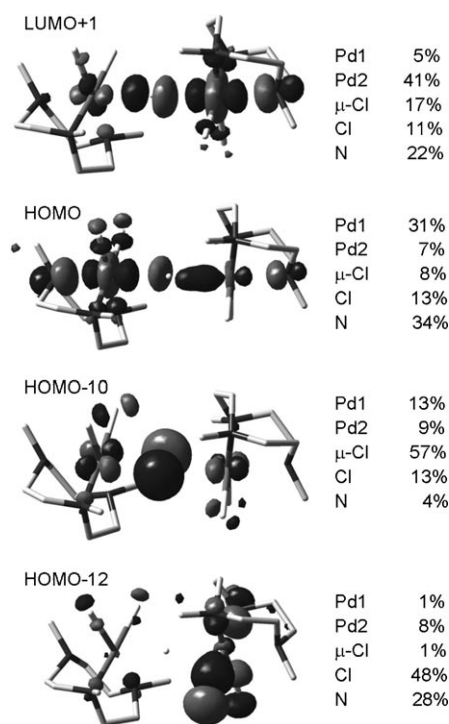


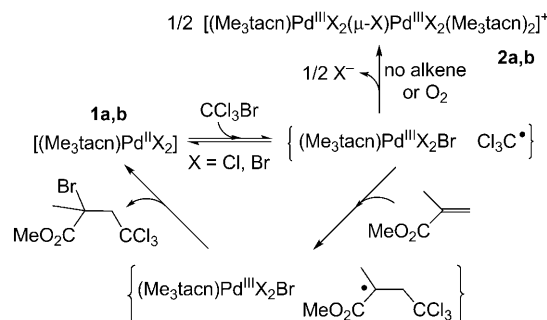
**Figure 3.** DFT-calculated (UB3LYP/CEP-31G) molecular orbitals (MOs) of **2a** that are proposed to be involved in the observed UV/Vis absorption bands. The calculated atomic contributions are listed for each MO (Pd1 and Pd2 represent the left and the right metal center, respectively,  $\mu$ -Cl is the bridging  $\text{Cl}^-$  ligand, Cl refers to the terminal  $\text{Cl}^-$  ligands, and N to the N atoms).<sup>[12]</sup>

lower energies of all transitions and thus supports the halide contributions to the corresponding MOs.<sup>[19b]</sup>

CV studies show that addition of one equivalent of halide to **1a** and **1b** leads to an increase of the peak current corresponding to the second oxidation wave (Figure 2, inset). CPE of **1a** at about 0.5 V versus  $\text{Fc}^+/\text{Fc}$  in the presence of 1 equiv of  $\text{Cl}^-$  led to the appearance of an intense band at 534 nm associated with the dinuclear species **2a**, followed by its complete disappearance to give a yellow solution after a two-electron oxidation (Figure 2).<sup>[12]</sup> While the yellow species is unstable at RT, it leads to formation of yellow crystals at  $-20^\circ\text{C}$  in  $\text{MeCN}/\text{Et}_2\text{O}$ . The crystal structure reveals a cationic mononuclear  $\text{Pd}^{\text{IV}}$  complex,  $[(\text{Me}_3\text{tacn})\text{Pd}^{\text{IV}}\text{Cl}_3](\text{PF}_6)$  (**3a**; Scheme 1); a similar complex  $[(\text{Me}_3\text{tacn})\text{Pd}^{\text{IV}}\text{Br}_3](\text{PF}_6)$  (**3b**) is obtained upon CPE of **1b** in the presence of 1 equiv of  $\text{Br}^-$ , both **3a** and **3b** exhibiting a pseudo-octahedral geometry around the Pd center (Figure 1c; Supporting Information, Figure S38).<sup>[12,27]</sup> The  $\text{Pd}^{\text{II}}/\text{Pd}^{\text{III}}/\text{Pd}^{\text{IV}}$  interconversions are reversible: electrochemical reduction of the mononuclear species **3a** (or **3b**) at  $-0.3$  V versus  $\text{Fc}/\text{Fc}^+$  occurs via the intermediate dinuclear complex **2a** (or **2b**) to eventually produce the mononuclear species **1a** (or **1b**). Interestingly, complexes **3a,b** are unstable and slowly decay to the corresponding  $\text{Pd}^{\text{III}}$  species **2a,b**; moreover, a rapid reaction occurs when 1 equiv of the  $\text{Pd}^{\text{II}}$  complex **1a** (or **1b**) is added to a solution of **3a** (or **3b**) to generate the dinuclear  $\text{Pd}^{\text{III}}$  complex **2a** (or **2b**) in quantitative yield. These studies suggest that the  $\text{Pd}^{\text{III}}$  complexes **2a,b** are more stable under

ambient conditions than either the corresponding  $\text{Pd}^{\text{IV}}$  species or a  $\text{Pd}^{\text{II}}/\text{Pd}^{\text{IV}}$  mixture that is equivalent to a mixed-valence  $\text{Pd}^{\text{IV}}\text{-X-Pd}^{\text{II}}$  species. This result is in contrast to the use of extreme conditions<sup>[8]</sup> or Pd-to-Ni substitution<sup>[19c,d]</sup> required for the generation of the  $\text{Pd}^{\text{III}}\text{-X-Pd}^{\text{III}}$  state in 1D chains. Furthermore, the interconversion between dinuclear  $\text{Pd}^{\text{III}}$  and mononuclear  $\text{Pd}^{\text{IV}}$  species parallels the proposed involvement of analogous intermediates in Pd-catalyzed C–H oxidative functionalization reactions and suggests that for a given ligand environment both types of intermediates can be present.<sup>[3–6]</sup>

The relatively low oxidation potentials of complexes **1a,b** have prompted us to investigate their reactivity in one-electron redox reactions, such as the Kharasch addition of polyhaloalkanes to alkenes.<sup>[28]</sup> Both **1a** and **1b** exhibit catalytic activity in the addition of  $\text{CCl}_3\text{Br}$  to a number of alkenes (methyl methacrylate, methyl acrylate, styrene, norbornene, cyclopentene) to give selectively the 1:1 addition product in good to high yields at  $65^\circ\text{C}$  under  $\text{N}_2$  (Supporting Information, Chart S1, Table S1).<sup>[12]</sup> Kinetic studies of the  $\text{CCl}_3\text{Br}$  addition to methyl methacrylate (MMA) catalyzed by **1a** reveal a first-order dependence on **1a** and MMA concentration and a saturation behavior with respect to  $\text{CCl}_3\text{Br}$  concentration, thus suggesting a mechanism that involves a reversible electron transfer/halogen transfer from  $\text{CCl}_3\text{Br}$  to  $\text{Pd}^{\text{II}}$  to form a  $\text{Pd}^{\text{III}}$  species and a  $\text{Cl}_3\text{C}^\bullet$  radical that subsequently reacts with the alkene and leads to the addition-product formation (Scheme 2).<sup>[28]</sup> While no  $\text{Pd}^{\text{III}}$



**Scheme 2.** Proposed mechanism for the Kharasch reaction catalyzed by **1a,b** and the formation of the dinuclear  $\text{Pd}^{\text{III}}$  complexes **2a,b**.

intermediate was observed under optimal catalytic conditions, the dinuclear complex **2a** was detected by UV/Vis at RT, both in absence and in presence of MMA (Supporting Information, Figure S24).<sup>[29]</sup> Moreover, a higher yield of **2a** (or **2b**) was obtained when **1a** (or **1b**) was reacted with  $\text{CCl}_3\text{Br}$  in presence of  $\text{O}_2$ , a known radical trap that can react with the  $\text{Cl}_3\text{C}^\bullet$  radical<sup>[30]</sup> and thus drive the formation of the dinuclear  $\text{Pd}^{\text{III}}$  species. As the catalytic reaction rate shows a first-order dependence in catalyst concentration, and the complex **2a** was not observed under optimal catalytic conditions, the formation of the dinuclear  $\text{Pd}^{\text{III}}$  complex is most likely a means of stabilizing the transient mononuclear  $\text{Pd}^{\text{III}}$  intermediate (Scheme 2).<sup>[12]</sup> Moreover, the observed chemical oxidation of **1a,b** to form **2a,b** suggests that the polyhaloal-

kane acts as both the oxidant and the halogen-atom donor and thus parallels the electrosynthesis of complexes **2a,b** through electrochemical oxidation in presence of an external halide (Scheme 1).<sup>[31]</sup>

In conclusion, we have presented herein the synthesis and characterization of stable dinuclear Pd<sup>III</sup> complexes formed by oxidation of mononuclear Pd<sup>II</sup> precursors. Effective stabilization of the Pd<sup>III</sup> oxidation state was accomplished using the common tridentate ligand Me<sub>3</sub>tacn and halide ions and does not require the formation of a Pd<sup>III</sup>–Pd<sup>III</sup> bond. Moreover, these dinuclear Pd<sup>III</sup> complexes seem to be more stable than the corresponding mononuclear Pd<sup>IV</sup> (and Pd<sup>III</sup>) complexes under an analogous ligand environment. These results support our hypothesis that Pd<sup>III</sup> complexes are more common than previously anticipated and can play important roles in various Pd-catalyzed reactions. Furthermore, we suggest that under a given ligand environment, the involvement of either Pd<sup>III</sup> or Pd<sup>IV</sup> species as reactive intermediates cannot be unambiguously ruled out or confirmed, given their facile interconversion. Moreover, the reported dinuclear Pd<sup>III</sup> complexes are models of the delocalized Pd<sup>III</sup>–X–Pd<sup>III</sup> electronic structure found in Group 10 M–X–M–X 1D extended chains. Current research efforts are aimed at characterizing the reactivity and electronic properties of these unique dinuclear systems.

Received: February 7, 2011  
Published online: May 9, 2011

**Keywords:** chain compounds · dinuclear complexes · Kharasch reaction · N ligands · palladium

- [1] E. Negishi, *Handbook of Organopalladium Chemistry for Organic Synthesis*, Wiley, Hoboken, NJ, **2002**.
- [2] a) K. Muñoz, *Angew. Chem.* **2009**, *121*, 9576; *Angew. Chem. Int. Ed.* **2009**, *48*, 9412; b) T. W. Lyons, M. S. Sanford, *Chem. Rev.* **2010**, *110*, 1147; c) A. J. Canty, *Dalton Trans.* **2009**, 10409; d) P. Sehnal, R. J. K. Taylor, I. J. S. Fairlamb, *Chem. Rev.* **2010**, *110*, 824.
- [3] a) D. C. Powers, T. Ritter, *Nat. Chem.* **2009**, *1*, 302; b) D. C. Powers, M. A. L. Geibel, J. Klein, T. Ritter, *J. Am. Chem. Soc.* **2009**, *131*, 17050.
- [4] N. R. Deprez, M. S. Sanford, *J. Am. Chem. Soc.* **2009**, *131*, 11234.
- [5] M. P. Lanci, M. S. Remy, W. Kaminsky, J. M. Mayer, M. S. Sanford, *J. Am. Chem. Soc.* **2009**, *131*, 15618.
- [6] J. R. Khusnutdinova, N. P. Rath, L. M. Mirica, *J. Am. Chem. Soc.* **2010**, *132*, 7303.
- [7] a) F. A. Cotton, I. O. Koshevoy, P. Lahuerta, C. A. Murillo, M. Sanau, M. A. Ubeda, Q. Zhao, *J. Am. Chem. Soc.* **2006**, *128*, 13674; b) F. A. Cotton, J. D. Gu, C. A. Murillo, D. J. Timmons, *J. Am. Chem. Soc.* **1998**, *120*, 13280.
- [8] a) S. Takaishi, M. Takamura, T. Kajiwarra, H. Miyasaka, M. Yamashita, M. Lwata, H. Matsuzaki, H. Okamoto, H. Tanaka, S. Kuroda, H. Nishikawa, H. Oshio, K. Kato, M. Takata, *J. Am. Chem. Soc.* **2008**, *130*, 12080; b) M. Yamashita, S. Takaishi, *Chem. Commun.* **2010**, 46, 4438.
- [9] a) A. J. Blake, L. M. Gordon, A. J. Holder, T. I. Hyde, G. Reid, M. Schröder, *J. Chem. Soc. Chem. Commun.* **1988**, 1452; b) G. Hunter, A. McAuley, T. W. Whitcombe, *Inorg. Chem.* **1988**, *27*, 2634; c) A. McAuley, T. W. Whitcombe, *Inorg. Chem.* **1988**, *27*, 3090; d) T. N. Margulis, L. J. Zompa, *Inorg. Chim. Acta* **1992**, *201*, 61; e) A. A. Sobanov, A. N. Vedernikov, G. Dyker, B. N. Solomonov, *Mendeleev Commun.* **2002**, *12*, 14.
- [10] A. J. Blake, A. J. Holder, Y. V. Roberts, M. Schröder, *J. Chem. Soc. Chem. Commun.* **1993**, 260.
- [11] a) K. Wieghardt, E. Schoeffmann, B. Nuber, J. Weiss, *Inorg. Chem.* **1986**, *25*, 4877; b) O. Schlager, K. Wieghardt, B. Nuber, *Inorg. Chem.* **1995**, *34*, 6449; c) A. J. Blake, I. A. Fallis, A. Heppeler, S. Parsons, S. A. Ross, M. Schröder, *J. Chem. Soc. Dalton Trans.* **1996**, 31; d) A. J. Blake, I. A. Fallis, S. Parsons, S. A. Ross, M. Schröder, *J. Chem. Soc. Dalton Trans.* **1996**, 525.
- [12] See the Supporting Information.
- [13] CCDC 809190 (**1a**), 809186 (**2a**, *T* = 100 K), 809187 (**2a**, *T* = 293 K), 809183 (**2b**), 809185 (**2c**), 809188 (**3a**), 809189 (**3b**), and 809184 ([[(Me<sub>3</sub>tacn)Pd<sup>II</sup>Cl(MeCN)]ClO<sub>4</sub>]) contain the supplementary crystallographic data for this paper. These data can be obtained free of charge from The Cambridge Crystallographic Data Centre via [www.ccdc.cam.ac.uk/data\\_request/cif](http://www.ccdc.cam.ac.uk/data_request/cif).
- [14] Coulometry measurements confirm that both oxidations correspond to one electron processes (see the Supporting Information).
- [15] The presence of dimers **2a** and **2b** in solution was confirmed by ESI-MS and the lack of an EPR signal for the corresponding solutions at 77 K or RT.
- [16] The presence of [(Me<sub>3</sub>tacn)PdCl(MeCN)]<sup>+</sup> in solution after one-electron oxidation of **1a** was detected by CV and confirmed by independent synthesis (see the Supporting Information). If (Me<sub>3</sub>tacn)PdCl(MeCN)<sup>+</sup> is the only halide abstraction product, then the theoretical yield of **2a** is 67%.
- [17] The high extinction coefficients of **2a,b** enable the unique visualization of mass-transport processes at the disk electrode during CV of **1a,b** (Supporting Information, Figure S15).
- [18] J. Terheijden, G. van Koten, D. M. Grove, K. Vrieze, A. L. Spek, *J. Chem. Soc. Dalton Trans.* **1987**, 1359.
- [19] a) K. Toriumi, Y. Wada, T. Mitani, S. Bandow, M. Yamashita, Y. Fujii, *J. Am. Chem. Soc.* **1989**, *111*, 2341; b) M. Yamashita, T. Manabe, K. Inoue, T. Kawashima, H. Okamoto, H. Kitagawa, T. Mitani, K. Toriumi, H. Miyamae, R. Ikeda, *Inorg. Chem.* **1999**, *38*, 1894; c) S. Takaishi, H. S. Wu, J. X. Xie, T. Kajiwarra, B. K. Breedlove, H. Miyasaka, M. Yamashita, *Inorg. Chem.* **2010**, *49*, 3694; d) M. Yamashita, T. Ishii, H. Matsuzaka, T. Manabe, T. Kawashima, H. Okamoto, H. Kitagawa, T. Mitani, K. Marumoto, S. Kuroda, *Inorg. Chem.* **1999**, *38*, 5124.
- [20] M. B. Robin, P. Day, *Adv. Inorg. Chem. Radiochem.* **1968**, *10*, 247.
- [21] No positional disorder along the Pd–(μ-X)–Pd axis was found for the bridging halide in the structures of either **2a** (both at RT and 100 K) or **2b,c** (see the Supporting Information).
- [22] For example, the Pd···Pd distance of the only known Pd<sup>III</sup>–Br–Pd<sup>III</sup> 1D chain is 5.21 Å at 110 K (Ref. [8a]).
- [23] SQUID measurements of **2a** showed a negligible magnetic susceptibility in the 2–320 K range.
- [24] No other absorption bands were seen in the range 700–2200 nm.
- [25] B. S. Brunschwig, C. Creutz, N. Sutin, *Chem. Soc. Rev.* **2002**, *31*, 168.
- [26] Although the α HOMO is mainly localized on Pd1 whereas the α LUMO + 1 is mainly localized on Pd2, both α → α and β → β transitions have identical contributions to the TD-DFT calculated absorption bands (see the Supporting Information). Similar MMCT transitions have been proposed to exist in antiferromagnetically coupled dinuclear Cu<sup>II</sup> complexes: F. Tuczek, E. I. Solomon, *Coord. Chem. Rev.* **2001**, *219*, 1075.
- [27] Only a limited number of cationic Pd<sup>IV</sup> complexes have been structurally characterized to date: a) K. Toriumi, M. Yamashita, H. Ito, T. Ito, *Acta Crystallogr. Sect. C* **1986**, *42*, 963; b) P. K. Byers, A. J. Canty, B. W. Skelton, A. H. White, *J. Chem. Soc. Chem. Commun.* **1987**, 1093; c) P. K. Byers, A. J. Canty, B. W. Skelton, A. H. White, *Organometallics* **1990**, *9*, 826;



- d) A. Bayler, A. J. Canty, P. G. Edwards, B. W. Skelton, A. H. White, *J. Chem. Soc. Dalton Trans.* **2000**, 3325; e) A. J. Canty, M. J. G. Hettinga, J. Patel, M. Pfeffer, B. W. Skelton, A. H. White, *Inorg. Chim. Acta* **2002**, 338, 94; f) W. Oloo, P. Y. Zavalij, J. Zhang, E. Khaskin, A. N. Vedernikov, *J. Am. Chem. Soc.* **2010**, 132, 14400.
- [28] a) R. A. Gossage, L. A. van de Kuil, G. van Koten, *Acc. Chem. Res.* **1998**, 31, 423; b) L. A. van de Kuil, D. M. Grove, R. A. Gossage, J. W. Zwikker, L. W. Jenneskens, W. Drenth, G. van Koten, *Organometallics* **1997**, 16, 4985.
- [29] While other Pd<sup>II</sup> complexes have been reported as catalysts for the Kharasch reaction, no Pd<sup>III</sup> intermediates have been detected to date: a) J. Tsuji, K. Sato, H. Nagashima, *Tetrahedron* **1985**, 41, 393; b) D. Motoda, H. Kinoshita, H. Shinokubo, K. Oshima, *Adv. Synth. Catal.* **2002**, 344, 261; c) A. S. Dneprovskii, A. A. Ermoshkin, A. N. Kasatochkin, V. P. Boyarskii, *Russ. J. Org. Chem.* **2003**, 39, 933.
- [30] P. Neta, J. Grodkowski, A. B. Ross, *J. Phys. Chem. Ref. Data* **1996**, 25, 709.
- [31] Chemical oxidation of **1b** with 0.5 equiv Br<sub>2</sub> generates **2b** in 40% yield (see the Supporting Information). No Pd<sup>IV</sup> complexes were detected during chemical oxidation with excess Br<sub>2</sub> or CCl<sub>3</sub>Br.